
MaskDiffusion: Boosting Text-to-Image Consistency with Conditional Mask

Yupeng Zhou¹ Daquan Zhou² Zuo-Liang Zhu¹ Yaxing Wang¹
Qibin Hou^{1*} Jiashi Feng²

¹VCIP, School of Computer Science, Nankai University

²ByteDance, Singapore

{ypzhousdu, andrewhou}@gmail.com

Abstract

Recent advancements in diffusion models have showcased their impressive capacity to generate visually striking images. Nevertheless, ensuring a close match between the generated image and the given prompt remains a persistent challenge. In this work, we identify that a crucial factor leading to the text-image mismatch issue is the inadequate cross-modality relation learning between the prompt and the output image. To better align the prompt and image content, we advance the cross-attention with an adaptive mask, which is conditioned on the attention maps and the prompt embeddings, to dynamically adjust the contribution of each text token to the image features. This mechanism explicitly diminishes the ambiguity in semantic information embedding from the text encoder, leading to a boost of text-to-image consistency in the synthesized images. Our method, termed MaskDiffusion, is training-free and hot-pluggable for popular pre-trained diffusion models. When applied to the latent diffusion models, our MaskDiffusion can significantly improve the text-to-image consistency with negligible computation overhead compared to the original diffusion models.

1 Introduction

Diffusion models [15, 9, 46, 49, 44] have been the most prevailing methods amongst generative methods, revealing its superiority in a variety of down-streaming tasks [2, 6, 31, 20, 45, 19, 41]. Recent state-of-the-art text-to-image (T2I) generation models (e.g., Imagen [36], DALL·E 2 [32] and Stable Diffusion [34]) are all based on diffusion process via iterative denoising steps. Benefiting from a mountain of training data, these methods have achieved great performance, and also attract tremendous attention from both academia and industry.

In the context of T2I diffusion models, despite the great progress, the inconsistency between the text prompt and the generated image is a severe problem [4]. To address this issue, lots of previous works [36, 32, 1] scale up diffusion models along with text encoders to achieve better performance but bring in huge extra computational burden. In this paper, to advocate the sustainable and green AI principle, we follow the principle that “*Entities must not be multiplied beyond necessity.*” Our goal is to resolve the drawbacks of existing diffusion models, such as missing objects and mismatched attributes (see Fig. 1), without introducing additional computational cost and extra data.

We get inspiration from the prompt-to-prompt work [13], which shows that cross-attention is the key component bridging the text prompt and the generated image. This motivates us to delve into the cross-attention mechanism to find a solution to the problem of text-to-image inconsistency as

*Corresponding author.



Figure 1: Different types of bad cases in Stable Diffusion and the corresponding cross-attention maps. The numerical score for each cross-attention map is computed by averaging the top 25% attention values. (a) Both “horse” and “dog” do not have a semantic relationship but suffer from overlapping attentive region problems, which leads to the “dog” neglect. (b) There is a large difference between the attention scores of “elephant” and “glasses”, leading to the missing of “glasses.” (c) The attentive regions of “Yellow” appear at the wrong position, resulting in the generation of a yellow bird. (d) Our results.

mentioned above. Through revisiting the cross-attention mechanism, we find that the main reason preventing T2I diffusion models from generating consistent images with the given prompt is the inadequate cross-modality relation learning. For example, as shown in the visualized cross-attention maps in Fig. 1, the objects or attributes often have attentive regions, but they cannot successfully appear in the resulting images.

To make the resulting image better match the text prompt, we propose MaskDiffusion, a training-free method that can boost the text-to-image consistency. MaskDiffusion renovates the vanilla cross attention by introducing a mask to i) prevent the semantic competition (See Fig. 1) in the cross attention maps, and ii) balance the attention value differences of different tokens. We conduct comprehensive experiments with Stable Diffusion [34] and compare them with four recent state-of-the-art methods. The results reveal the superiority of MaskDiffusion over other methods in generating images highly consistent with the text prompt.

2 Related Work

Diffusion models [34, 36, 14, 32, 29] are predominate in the context of image generation, outperforming GANs [12, 10, 18], VAEs [28, 40, 33], and normalized flows [26, 7] in fidelity and diversity. Since the classifier-free guidance [16] and the conditioning mechanism based on cross attention [34] were proposed, conditional generation under diverse types of guidance becomes practical, benefiting to numerous related tasks, including super resolution [37], inpainting [23, 43], layout-to-image generation [48, 8] and text-to-image (T2I) generation [36, 32, 1]. Amongst these tasks, T2I diffusion models attract the most significant attention, leading to creative and aesthetic applications [27, 47].

For T2I diffusion models, a core demand is the consistency between the prompts and the generated images. However, the existing T2I diffusion models fail to maintain such consistency in some cases [36], especially when the prompt is extremely long or involves multiple concepts, hindering further application. To alleviate this issue, Composable Diffusion [22] makes the first step, which takes advantage of the characteristics of classifier-free guidance and enables limited operators (i.e., and, not) to achieve better text-to-image alignment. However, its ability is highly constrained by the limited operators, and it is unsuitable for a fine-grained adjustment. More recent works can be

partitioned into two groups. They either mine semantic correspondence via cross attention or utilize extra guidance (e.g., layout, silhouette) with or without finetuning the input latent code.

In term of extra guidance, most of works [42, 5, 24] utilize layout provided by humans as prior. The layout, as a strong prior of position, leads to a strong ability to locate multiple objects of these methods. Additionally, [42] trains a layout predictor to handle cases while the layout mentioned above is absent. However, when the number of objects is large, it is burdensome to assign a layout for each one, and training another network is not an optimal solution as well.

Another category of methods are derived from prompt-to-prompt [13], which figures out the strong connection between the generated object and the cross-attention map. Attend-and-Excite [4] utilizes cross attention to optimize the latent code on the fly, whose performance is promising but speed is slow, due to the optimization. Instead, our method is plug-and-play without any latent optimization, which only modifies the cross-attention map during the denoising process. Some concurrent works share a similar idea about attention layer manipulation. A brief comparison between our method and theirs is presented below, and the detailed technique differences are discussed in Sec. 3. The Structure Diffusion [11] modifies the value in the qkv attention operation and needs substantial extra queries to the text encoder, resulting in a surge of computational consumption. The aim of [25] is to guarantee the size and position of objects, while our method focuses on missing objects and attribute mismatch. Attributing to our laborious designs, Our method solves the consistency issue with minimal consumption increase and higher efficiency.

3 Method

Our objective is to address the issues presented in current diffusion models, like missing objects and mismatched attributes, without extra training. Prior to delving into the methodology for enhancing the conformity of generated images with the provided text prompt, it is imperative to revisit the concept of cross-attention within text-to-image diffusion models.

3.1 Revisiting Cross-Attention

The cross-attention in Stable Diffusion establishes a connection between the L -token encoded prompt $P \in \mathbb{R}^{L \times D}$ and N -pixel intermediate noise $x_t \in \mathbb{R}^{N \times D}$ by computing the similarities between the text tokens and the image features as follows:

$$\text{Attention}(x_t, P) = \text{Softmax}\left(\frac{Q(x_t)K(P)^T}{\sqrt{D}}\right), \quad (1)$$

where Q and K are linear transformations and D is the channel dimension. For simplicity, we use $C \in \mathbb{R}^{N \times L}$ to denote the resulting attention map. Though attention maps can reflect where an object will be located as demonstrated in [4], they cannot guarantee the text-to-image consistency.

Given a picked token set, we expect to visualize the cross attention map for each picked token. For each picked $token_i$, we extract the cross attention map $C_i \in \mathbb{R}^N$ from $C \in \mathbb{R}^{N \times L}$ at each step and average all the cross attention maps to visualize the attentive regions. After analyzing the bad cases of Stable Diffusion and the corresponding cross attention maps, we find that the attention values in the attention maps are closely related to text-to-image consistency. Basically, the common bad cases can be categorized into three types, which are shown in the Fig. 1 and summarized below:

- **Overlapping Attentive Regions.** When two objects without a semantic relationship overlap in the attention maps and their attention values are close, there will be semantic conflict. In this case, the diffusion model will ignore one of the objects. For example, in Fig. 1(a), there is no semantic relationship between horse and dog, and hence the diffusion model ignores dog and only generates horse.
- **Preempted Attentive Regions.** In this case, the attentive regions of two objects appear at correct positions but there is a large difference between their attention values. For example, in Fig. 1(b), the attention score of “elephant” is much higher than that of “glasses.” Consequently, “glasses” does not appear in the generated image.
- **Wrong Attentive Regions.** This means that the attribute appears at a wrong position, which makes the attribute be expressed on other objects. As shown in Fig. 1(c), the “yellow” attribute is reflected on the “bird” object.

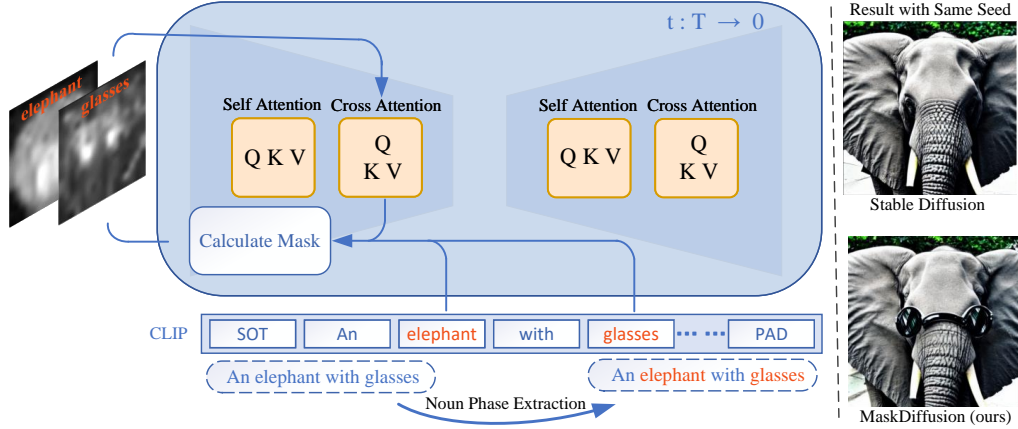


Figure 2: The overall pipeline of MaskDiffusion. The object tokens and their attributes are extracted from prompts before the diffusion process. For each diffusion sample time step, we calculate a mask of cross attention for the object tokens and their attributes to improving the image-text consistency.

3.2 Conditional Mask for Text-to-Image Consistency

Regarding the aforementioned analysis, we propose a simple and intuitive solution by adding a mask conditioned on the text prompt embeddings and the cross-attention maps. Given the intermediate features x_t and encoded prompt P , we reformulate the cross-attention via the following formula:

$$\text{CrossAttn}(x_t, P) = \text{Softmax} \left(\frac{Q(x_t)K(P)^T}{\sqrt{D}} + M \right) V(P) \quad (2)$$

where $M \in \mathbb{R}^{N \times L}$ is a mask. Now, we describe how to generate the mask.

Algorithm 1 Adaptive Mask Generation

Input: the prompt $P \in \mathbb{R}^{L \times D}$, the picked tokens set S , a zeroed mask $M \in \mathbb{R}^{N \times L}$, $w_0 = 5$

- 1: **for** $token_i$ in set S **do**
- 2: Using the region selection algorithm to find pixels related to the token and putting them into region R_i
- 3: **for** $pixel_j$ in R_i **do**
- 4: $M_{ji} \leftarrow M_{ji} + w_0$
- 5: **end for**
- 6: **end for**

Output: Mask $M \in \mathbb{R}^{L \times N}$ which will be used for improving text-to-image consistency

Given a set of picked tokens S , we use the token embeddings to strengthen the semantic information of the image features under the help of the mask. The complete mask generation process is summarized in Algorithm 1. The core is a region selection algorithm, which is described below.

Region Selection. The region selection algorithm finds out the pixels from the attention map $C_i \in \mathbb{R}^N$ associated with a certain $token_i$, which is the key of adaptive mask generation. We define the region selection process as an optimization problem. It helps select regions with high response values and meanwhile avoid the overlapping problem as mentioned in Sec. 3.1. In mathematical form, we select regions R_1, R_2, \dots, R_S for the picked tokens $token_1, token_2, \dots, token_S$ by maximizing the following objective function F_θ :

$$\max \left(\sum_{i=0}^S \text{sum}(R_i) - \lambda \sum_{i=0}^S \sum_{j=0}^S \text{sum}(R_i \cap R_j) \right), \quad (3)$$

s.t. $\forall \text{pixel} \in R_i, C_i[\text{pixel}] \geq \tau_i, \quad i = 1, 2, \dots, L$

where S is the number of picked tokens and $\text{sum}(\cdot)$ means accumulating the attention value of each pixel in its corresponding region.

Finding the optimal solution to this optimization objective is difficult in that its second term contains the interaction of different regions. To resolve this, we simplify the second term of the optimization objective and solve an approximate optimization objective as follows. We first select the top k largest attention values from the cross attention map associated with each token as the approximate regions A_1, A_2, \dots, A_S for the picked tokens. After that, we simplify the above optimization objective into the following formula by the approximate regions:

$$\max \left(\sum_{i=0}^S \text{sum}(R_i) - \lambda \sum_{i=0}^S \sum_{j=0}^S \text{sum}(R_i \cap A_j) \right). \quad (4)$$

The new optimization objective eliminates the correlation between regions R_1, R_2, \dots, R_S . We do not need to consider other regions when solving for some region R_i . Therefore, it can be solved very quickly. By default, we set the value of λ to 0.5.

In practice, we apply a Gaussian filter over the cross-attention maps as done in [4]. Then, for the cross-attention map associated with each token after Gaussian smoothing, we select positions whose attention values are larger than 0.5 times of the largest attention value. The advantages of these operations are two-fold. First, it can help erase those regions corresponding to other objects with low attention values. Second, the highest attention values in attention maps associated with different tokens may have a large difference. For example, in Fig. 1(b), the attention score of “elephant” (0.1247) is much larger than that of “glasses” (0.0117). The above operation can help adaptively select proper attentive regions.

Updating Cross-Attention Maps with Momentum. The optimization objective discussed above solely focuses on adjusting the cross-attention map at the current time step, which may result in unstable masked positions across different time steps. We solve this issue by introducing a momentum along the time step dimension. Specifically, for time step t , we update C^t by combining the cross-attention maps C^t and C^{t+1} as follows:

$$C^t \leftarrow \alpha C^{t+1} + \beta C^t, \quad (5)$$

where α and β are the coefficients to adjust the effects of two adjacent time steps. Here, we empirically set $\alpha = 0.03$ and $\beta = 0.99$.

Overall Pipeline. Given a text prompt, our approach involves initially extracting all nouns and adjectives corresponding to the objects present within the visual content, utilizing the SpaCy library [17]. During the sampling process, we employ the pre-trained U-Net [35] network from Stable Diffusion for denoising at each time step, while applying a mask to the cross-attention block. Specifically, the mask M is computed using Algorithm 1 of the cross-attention map, focusing on selected tokens such as object nouns and their associated attributes.

To optimize computational efficiency during inference, we solely compute the attention mask pertaining to the extracted nouns and adjectives, disregarding other text tokens. The mask is exclusively applied to feature maps with a resolution of 16×16 . A detailed analysis of the impact of feature resolutions can be found in Section 4.6 and Figure 6.

4 Experiment

4.1 Implementation Details

We implement our method based on version 1.4 of Stable Diffusion [34] pre-trained on the LAION-5B [38]. Since our method is training-free, we do not update any parameters of Stable Diffusion. In all experiments, the size of the image generated by our model and the comparison model is 512×512 . Our test prompts include simple sentences and complex sentences. We sample some prompts from MS-COCO [21] and synthesize some prompts according to the specified format based on GPT [3] to further enhance the diversity of our test data, including the following formats: 1) a [animal/object A] and a [animal/object B], like “A cat and a dog”. 2) a [color/material A][object/animal A] and a [color/material B][object/animal B], like “a red bus and a white dog”. 3) More complex sentences: interactions involving more than three objects, like “A happy dog wagging its tail while fetching a stick in a pond”. More details are described in the supplementary material.

4.2 Model Efficiency

We conduct an inference time comparison of five models in this subsection. We generate images using the same 50 prompts and random seeds and take the average inference time for a fair comparison. The five method names and their corresponding inference time are listed in Tab. 1.

Composable Diffusion [22] divides prompt into concepts and composes diffusion models with all concepts. Consequently, the denoising model is employed multiple times within a single sampling time step to calculate different concepts, resulting in a time-consuming process. Structured Diffusion [11], on the other hand, splits the sentence into several parts and employs the CLIP text encoder to obtain an embedding. As the CLIP text encoder is queried multiple times, there is a slight increase in inference time. Among the five models, Attend-and-Excite [4] exhibits the slowest inference speed, primarily due to the iterative optimization within a single sampling time step. Our model only introduces a mask conditioned on the prompt embeddings and hence achieves almost the same performance as the original Stable Diffusion, which demonstrates the efficiency of our method.

Table 1: Quantitative comparison of our MaskDiffusion with Stable Diffusion [34], ComposeDiffusion [22], Structure Diffusion [11], Attend-and-Excite [4]. We give the average inference time, user’s supporting rate for simple prompts and complex prompts, and CLIP score similarity to fully measure the performance of models.

Model	Inference Time	Simple Prompt Supporting Rate	Complex Prompt Supporting Rate	CLIP Score
Stable Diffusion [34]	81s	3.10%	9.16%	26.16
ComposableDiffusion [22]	126s	0.20%	2.29%	26.59
Structure Diffusion [11]	88s	0.58%	2.87%	25.82
Attend-and-Excite [4]	215s	12.96%	11.24%	26.33
MaskDiffusion (ours)	81s	83.16%	74.77%	26.82

4.3 Visual Comparison

We compare our model with other four diffusion-based generative models, including Stable Diffusion [34], Composable Diffusion [22], Structured Diffusion [11], and Attend-and-Excite [4]. We evaluate the matching degree of images generated by different models and prompts using the same seed. The prompts and generated images are shown in Fig. 3. Because Attend-and-Excite is the most competitive comparison model among them, we perform an additional comparison with it in Fig. 4. Through a visual comparison of the generated images, we can see that our model produces the most realistic and text-to-image consistent results. We can also observe that our results are very similar to those produced by the vanilla Stable Diffusion and improve the consistency between the prompts and images. More examples can be found in our supplementary materials.

4.4 CLIP Score Comparison

Here, we use CLIP score similarity to quantitatively evaluate the performance of our model. Considering the limitations of CLIP score for semantic understanding [39], we remove sentences that are extremely long or contain complex interactions between multiple objects during evaluation. For a fair comparison, we conduct experiments with multiple random seeds and calculate the CLIP score similarity of five models. The results are shown in Tab. 1.

4.5 User Study

Here, we conduct a user study to analyze the fidelity of the images generated by our MaskDiffusion and four recent methods. We randomly sample 30 prompts and use the same random seed to generate images using the five models. The selected prompts include 50% simple prompts, containing two words and attributes, and 50% complex prompts, containing interactions of more than three objects. The order of the models is shuffled and the participants were not informed which images are generated by some certain model for a fair comparison.

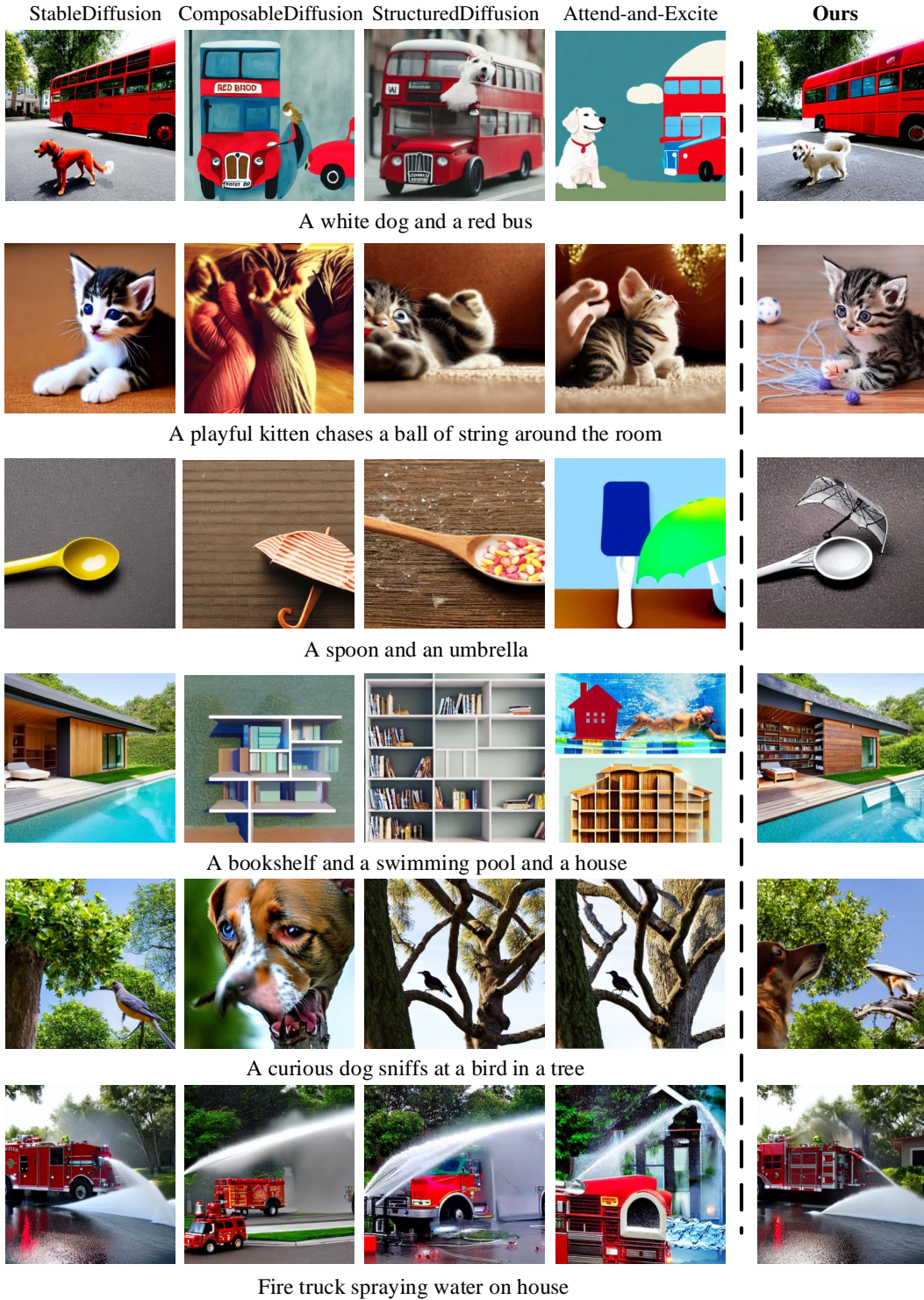


Figure 3: Visual comparison of MaskDiffusion with Stable Diffusion [34], Composable Diffusion [22], Structured Diffusion [11], and Attend-and-Excite [4]. It can be seen from the generated images that our method achieves the best performance among all the five models.

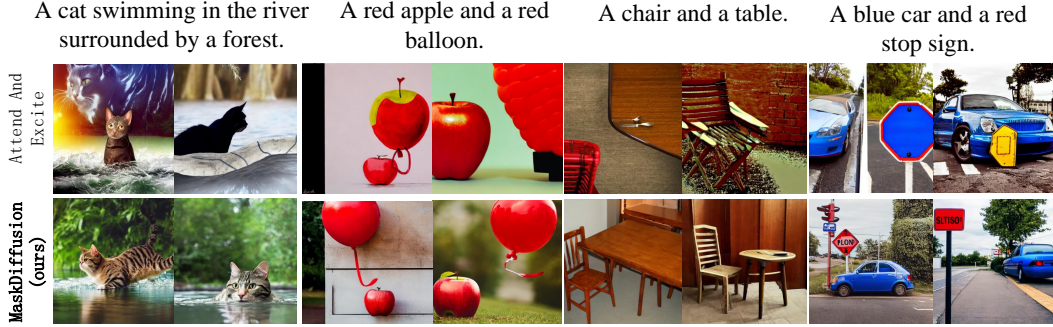


Figure 4: Additional comparisons with the recent Attend-and-Excite [4] using the same set of seeds for each prompt. We can see that our method can achieves a better consistency between the text prompt and the generated images.

We asked 35 participants to choose the most similar image to the prompt based on three points: 1) Whether the objects mentioned in the prompt appear. 2) Whether the attributes of the object are correct. 3) Whether the generated image is real and natural. We count the users’ votes and define it as the user’s support rate. We show the results in Tab. 1. As can be seen, our MaskDiffusion can achieve overwhelming user approval no matter how complex the sentences are.

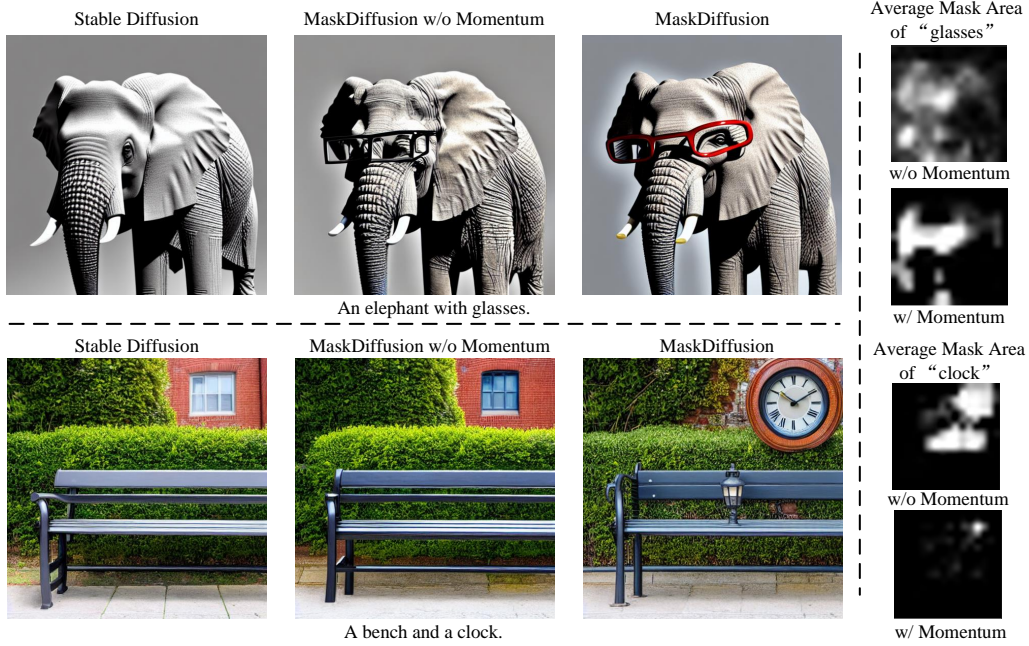


Figure 5: Ablation analysis on the momentum updating strategy. We compare with the original Stable Diffusion and our MaskDiffusion without momentum updating.

4.6 Ablation Study

In this subsection, we conduct some ablation analysis to help readers better understand the proposed method.

Updating Cross-Attention Maps with Momentum. We update cross-attention maps with momentum as explained in Sec. 3.2. It takes the information of the previous time step into consideration to make the generated mask more stable. To show the effect of this operation, we design a set of ablation experiments, namely the original Stable Diffusion, MaskDiffusion without momentum updating, and

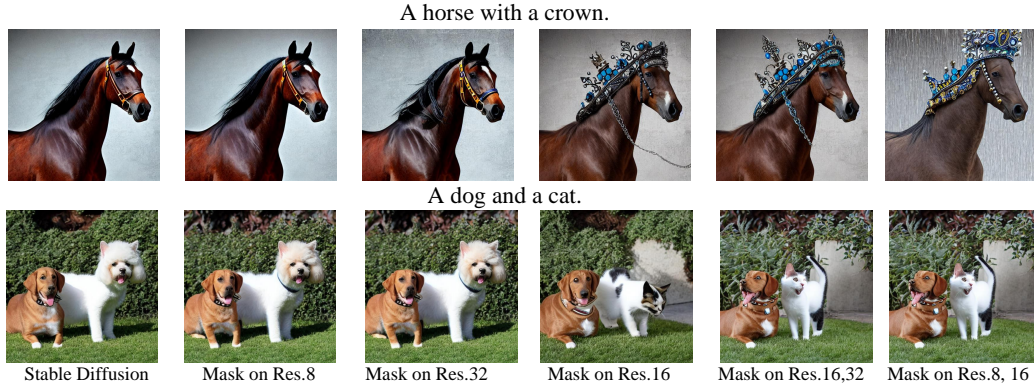


Figure 6: Ablation study of adding mask on cross attention of different resolution features. “res.” is an abbreviation for resolution. For example, “res.8” stands for 8×8 resolution U-Net features. It can be clearly seen that generating a mask based on the 16×16 features plays a decisive role in the success of our MaskDiffusion.

our MaskDiffusion, and show the results in Fig. 5. We also record the mask at each time step and compute the averaged mask for each token in the right part of Fig. 5. From the figure, we can see that without the momentum updating strategy, some of the objects may be missing in the resulting images. On the contrary, our MaskDiffusion can well address this issue.

Masks Generated at Different Resolutions. The diffusion model adopts a hierarchical structure, i.e., the UNet. In Stable Diffusion, the cross-attention is computed based on features at each feature level. In order to clarify which resolution is more appropriate to add masks, we conduct ablation experiments by adding masks to cross-attentions of different resolutions. As shown in Fig. 6, we can observe that the 16×16 resolution plays an important role in the success of our method. A reasonable explanation is that during CLIP training, the text and image embeddings are aligned. The resolution of the output image embeddings in CLIP is 14×14 and the 16×16 resolution features in U-Net is close to it.

5 Conclusions

In this paper, we have conducted extensive research on the image-text mismatch problem of the text-to-image diffusion model, revealing the correlation between the inappropriate attention value of the cross-attention map and the image-text mismatch problem. To amend the inappropriate attention value, we introduced an adaptive mask to control the attention value of the cross-attention map, conditioned on the cross-attention map and prompt semantics. Based on this, we propose a simple and training-free method called MaskDiffusion to generate high-quality images with high text-to-image consistency. Under extensive experiments, our MaskDiffusion achieves better text-to-image consistency with low cost compared to the original diffusion models. We believe that our work provides a valuable contribution to the field of text-to-image synthesis. we hope that it can be used to improve the performance of future text-to-image synthesis models.

Limitations. The main limitation of our method arises from the CLIP text encoder [30]. Our method can adaptively add masks based on the cross-attention map and CLIP semantics, while the descriptive capacity of the CLIP text encoder for complex sentences may be limited, leading to ambiguous or incorrect semantics. For instance, when evaluating the prompt “A green book in a pink basket.”, we found that CLIP misunderstands the sentence, as evidenced by the higher cosine similarity between “basket” and “green” compared to “basket” and “pink.” The ambiguous semantics can confuse the diffusion generation process, which we plan to address in our future work.

References

- [1] Yogesh Balaji, Seungjun Nah, Xun Huang, Arash Vahdat, Jiaming Song, Qinsheng Zhang, Karsten Kreis, Miika Aittala, Timo Aila, Samuli Laine, Bryan Catanzaro, Tero Karras, and Ming-Yu Liu. ediff-i: Text-to-image diffusion models with an ensemble of expert denoisers. *arXiv preprint*, 2023. 1, 2
- [2] Manuel Brack, Patrick Schramowski, Felix Friedrich, Dominik Hintersdorf, and Kristian Kersting. The stable artist: Steering semantics in diffusion latent space. *arXiv preprint*, 2022. 1
- [3] Tom Brown, Benjamin Mann, Nick Ryder, Melanie Subbiah, Jared D Kaplan, Prafulla Dhariwal, Arvind Neelakantan, Pranav Shyam, Girish Sastry, Amanda Askell, et al. Language models are few-shot learners. *Adv. Neural Inform. Process. Syst.*, 2020. 5
- [4] Hila Chefer, Yuval Alaluf, Yael Vinker, Lior Wolf, and Daniel Cohen-Or. Attend-and-excite: Attention-based semantic guidance for text-to-image diffusion models. *arXiv preprint*, 2023. 1, 3, 5, 6, 7, 8
- [5] Minghao Chen, Iro Laina, and Andrea Vedaldi. Training-free layout control with cross-attention guidance. *arXiv preprint*, 2023. 3
- [6] Rui Chen, Yongwei Chen, Ningxin Jiao, and Kui Jia. Fantasia3d: Disentangling geometry and appearance for high-quality text-to-3d content creation. *arXiv preprint*, 2023. 1
- [7] Ricky T. Q. Chen, Jens Behrmann, David Duvenaud, and Jörn-Henrik Jacobsen. Residual flows for invertible generative modeling. In *Adv. Neural Inform. Process. Syst.*, 2019. 2
- [8] Jiaxin Cheng, Xiao Liang, Xingjian Shi, Tong He, Tianjun Xiao, and Mu Li. Layoutdiffuse: Adapting foundational diffusion models for layout-to-image generation. In *IEEE Conf. Comput. Vis. Pattern Recog.*, 2023. 2
- [9] Prafulla Dhariwal and Alexander Nichol. Diffusion models beat gans on image synthesis. In *Adv. Neural Inform. Process. Syst.*, 2021. 1
- [10] Patrick Esser, Robin Rombach, and Björn Ommer. Taming transformers for high-resolution image synthesis. In *IEEE Conf. Comput. Vis. Pattern Recog.*, 2021. 2
- [11] Weixi Feng, Xuehai He, Tsu-Jui Fu, Varun Jampani, Arjun Akula, Pradyumna Narayana, Sugato Basu, Xin Eric Wang, and William Yang Wang. Training-free structured diffusion guidance for compositional text-to-image synthesis. In *Int. Conf. Learn. Represent.*, 2023. 3, 6, 7
- [12] Ian Goodfellow, Jean Pouget-Abadie, Mehdi Mirza, Bing Xu, David Warde-Farley, Sherjil Ozair, Aaron Courville, and Yoshua Bengio. Generative adversarial networks. *Communications of the ACM*, 2020. 2
- [13] Amir Hertz, Ron Mokady, Jay Tenenbaum, Kfir Aberman, Yael Pritch, and Daniel Cohen-Or. Prompt-to-prompt image editing with cross attention control. *arXiv preprint*, 2022. 1, 3
- [14] Jonathan Ho, Ajay Jain, and Pieter Abbeel. Denoising diffusion probabilistic models. In *Adv. Neural Inform. Process. Syst.*, 2020. 2
- [15] Jonathan Ho, Chitwan Saharia, William Chan, David J Fleet, Mohammad Norouzi, and Tim Salimans. Cascaded diffusion models for high fidelity image generation. *arXiv preprint*, 2021. 1
- [16] Jonathan Ho and Tim Salimans. Classifier-free diffusion guidance. *arXiv preprint*, 2022. 2
- [17] Matthew Honnibal and Ines Montani. spaCy 2: Natural language understanding with Bloom embeddings, convolutional neural networks and incremental parsing. To appear, 2017. 5
- [18] Minguk Kang, Jun-Yan Zhu, Richard Zhang, Jaesik Park, Eli Shechtman, Sylvain Paris, and Taesung Park. Scaling up gans for text-to-image synthesis. In *IEEE Conf. Comput. Vis. Pattern Recog.*, 2023. 2
- [19] Bahjat Kawar, Shiran Zada, Oran Lang, Omer Tov, Huiwen Chang, Tali Dekel, Inbar Mosseri, and Michal Irani. Imagic: Text-based real image editing with diffusion models. In *IEEE Conf. Comput. Vis. Pattern Recog.*, 2023. 1
- [20] Nupur Kumari, Bingliang Zhang, Richard Zhang, Eli Shechtman, and Jun-Yan Zhu. Multi-concept customization of text-to-image diffusion. In *IEEE Conf. Comput. Vis. Pattern Recog.*, 2023. 1
- [21] Tsung-Yi Lin, Michael Maire, Serge Belongie, James Hays, Pietro Perona, Deva Ramanan, Piotr Dollár, and C Lawrence Zitnick. Microsoft coco: Common objects in context. In *Eur. Conf. Comput. Vis.*, 2014. 5
- [22] Nan Liu, Shuang Li, Yilun Du, Antonio Torralba, and Joshua B Tenenbaum. Compositional visual generation with composable diffusion models. In *Eur. Conf. Comput. Vis.*, 2022. 2, 6, 7
- [23] Andreas Lugmayr, Martin Danelljan, Andres Romero, Fisher Yu, Radu Timofte, and Luc Van Gool. Repaint: Inpainting using denoising diffusion probabilistic models. In *IEEE Conf. Comput. Vis. Pattern Recog.*, 2022. 2
- [24] Wan-Duo Kurt Ma, J. P. Lewis, W. Bastiaan Kleijn, and Thomas Leung. Directed diffusion: Direct control of object placement through attention guidance. *arXiv preprint*, 2023. 3
- [25] Jiafeng Mao and Xueting Wang. Training-free location-aware text-to-image synthesis. *arXiv preprint*, 2023. 3
- [26] Siniša Šegvić Matej Grcić, Ivan Grubišić. Densely connected normalizing flows. *Adv. Neural Inform. Process. Syst.*, 2021. 2
- [27] Chong Mou, Xintao Wang, Liangbin Xie, Yanze Wu, Jian Zhang, Zhongang Qi, Ying Shan, and Xiaohu Qie. T2i-adapter: Learning adapters to dig out more controllable ability for text-to-image diffusion models. *arXiv preprint*, 2023. 2
- [28] Gaurav Parmar, Dacheng Li, Kwonjoon Lee, and Zhuowen Tu. Dual contradistinctive generative autoencoder. In *IEEE Conf. Comput. Vis. Pattern Recog.*, 2021. 2
- [29] William Peebles and Saining Xie. Scalable diffusion models with transformers. *arXiv preprint*, 2022. 2
- [30] Alec Radford, Jong Wook Kim, Chris Hallacy, Aditya Ramesh, Gabriel Goh, Sandhini Agarwal, Girish Sastry, Amanda Askell, Pamela Mishkin, Jack Clark, et al. Learning transferable visual models from natural language supervision. In *International Conference on Machine Learning (ICML)*, 2021. 9

- [31] Amit Raj, Srinivas Kaza, Ben Poole, Michael Niemeyer, Ben Mildenhall, Nataniel Ruiz, Shiran Zada, Kfir Aberman, Michael Rubenstein, Jonathan Barron, Yuanzhen Li, and Varun Jampani. Dreambooth3d: Subject-driven text-to-3d generation. 2023. 1
- [32] Aditya Ramesh, Prfulla Dhariwal, Alex Nichol, Casey Chu, and Mark Chen. Hierarchical text-conditional image generation with clip latents. *arXiv preprint*, 2022. 1, 2
- [33] Ali Razavi, Aaron van den Oord, and Oriol Vinyals. Generating diverse high-fidelity images with vq-vae-2. In *Adv. Neural Inform. Process. Syst.*, 2019. 2
- [34] Robin Rombach, Andreas Blattmann, Dominik Lorenz, Patrick Esser, and Björn Ommer. High-resolution image synthesis with latent diffusion models. In *IEEE Conf. Comput. Vis. Pattern Recog.*, 2022. 1, 2, 5, 6, 7
- [35] Olaf Ronneberger, Philipp Fischer, and Thomas Brox. U-net: Convolutional networks for biomedical image segmentation. In *Med. Image. Comput. Comput. Assist. Interv.*, 2015. 5
- [36] Chitwan Saharia, William Chan, Saurabh Saxena, Lala Li, Jay Whang, Emily L Denton, Kamyar Ghasemipour, Raphael Gontijo Lopes, Burcu Karagol Ayan, Tim Salimans, et al. Photorealistic text-to-image diffusion models with deep language understanding. *Adv. Neural Inform. Process. Syst.*, 2022. 1, 2
- [37] Chitwan Saharia, Jonathan Ho, William Chan, Tim Salimans, David J. Fleet, and Mohammad Norouzi. Image super-resolution via iterative refinement. *IEEE Trans. Pattern Anal. Mach. Intell.*, 2023. 2
- [38] Christoph Schuhmann, Romain Beaumont, Richard Vencu, Cade Gordon, Ross Wightman, Mehdi Cherti, Theo Coombes, Aarush Katta, Clayton Mullis, Mitchell Wortsman, et al. Laion-5b: An open large-scale dataset for training next generation image-text models. *arXiv preprint*, 2022. 5
- [39] Tristan Thrush, Ryan Jiang, Max Bartolo, Amanpreet Singh, Adina Williams, Douwe Kiela, and Candace Ross. Winoground: Probing vision and language models for visio-linguistic compositionality. In *IEEE Conf. Comput. Vis. Pattern Recog.*, 2022. 6
- [40] Aaron van den Oord, Oriol Vinyals, and koray kavukcuoglu. Neural discrete representation learning. In *Adv. Neural Inform. Process. Syst.*, 2017. 2
- [41] Zhendong Wang, Huangjie Zheng, Pengcheng He, Weizhu Chen, and Mingyuan Zhou. Diffusion-gan: Training gans with diffusion. *arXiv preprint*, 2022. 1
- [42] Qiucheng Wu, Yujian Liu, Handong Zhao, Trung Bui, Zhe Lin, Yang Zhang, and Shiyu Chang. Harnessing the spatial-temporal attention of diffusion models for high-fidelity text-to-image synthesis. *arXiv preprint*, 2023. 3
- [43] Shaoan Xie, Zhifei Zhang, Zhe Lin, Tobias Hinz, and Kun Zhang. Smartbrush: Text and shape guided object inpainting with diffusion model. *arXiv preprint*, 2022. 2
- [44] Xingqian Xu, Zhangyang Wang, Eric Zhang, Kai Wang, and Humphrey Shi. Versatile diffusion: Text images and variations all in one diffusion model. *arXiv preprint*, 2022. 1
- [45] Binxin Yang, Shuyang Gu, Bo Zhang, Ting Zhang, Xuejin Chen, Xiaoyan Sun, Dong Chen, and Fang Wen. Paint by example: Exemplar-based image editing with diffusion models. *arXiv preprint*, 2022. 1
- [46] Xingyi Yang, Daquan Zhou, Jiashi Feng, and Xinchao Wang. Diffusion probabilistic model made slim. In *IEEE Conf. Comput. Vis. Pattern Recog.*, 2023. 1
- [47] Lvmin Zhang and Maneesh Agrawala. Adding conditional control to text-to-image diffusion models. *arXiv preprint*, 2023. 2
- [48] Guangcong Zheng, Xianpan Zhou, Xuewei Li, Zhongang Qi, Ying Shan, and Xi Li. Layoutdiffusion: Controllable diffusion model for layout-to-image generation. In *IEEE Conf. Comput. Vis. Pattern Recog.*, 2023. 2
- [49] Daquan Zhou, Weimin Wang, Hanshu Yan, Weiwei Lv, Yizhe Zhu, and Jiashi Feng. Magicvideo: Efficient video generation with latent diffusion models. *arXiv preprint*, 2023. 1